

Damián H. Zanette · Sebastián Risau Gusmán

Infection spreading in a population with evolving contacts

Received: date / Accepted: date

Abstract We study the spreading of an infection within an SIS epidemiological model on a network. Susceptible agents are given the opportunity of breaking their links with infected agents. Broken links are either permanently removed or reconnected with the rest of the population. Thus, the network coevolves with the population as the infection progresses. We show that a moderate reconnection frequency is enough to completely suppress the infection. A partial, rather weak isolation of infected agents suffices to eliminate the endemic state.

Keywords SIS epidemics · Agent-based models · Evolving networks

PACS 87.23.Cc · 89.75.Hc · 87.23.Ge

1 Introduction

Outbursts of epidemics in human populations trigger individual and collective reactions that can substantially alter the social structure. As a consequence of risk perception, non-infected individuals may start avoiding contact with their infected equals, even when their previous relationship was fluent. The whole society could collectively decide to isolate its infected members until danger is overcome. More altruistic non-infected individuals may be tolerant of the contact with infected individuals but, in turn, the latter may discontinue the relationship to impede contagion. The escape from crowded cities during the Black Death in the late Middle Ages, documented in Giovanni Boccaccio's Decameron, and the closing of schools, churches, and theaters during influenza epidemics in the early twentieth century, constitute dramatic historical instances of such behaviours [1,2]. Quarantine protocols, and preventive isolation during leprosy or tuberculosis treatment, are present-day examples [3]. In any case, these changes in the pattern of social contacts help to limit and control the incidence of the infection.

In this paper, we explore the effects of an evolving pattern of contacts on the dynamics of infection spreading, in the framework of a simple epidemiological model. We consider a population of agents whose pattern of contacts is represented by a network. If a link of the network joins two agents, contagion is possible when one of them is infected and his neighbour is not. To account for the social processes addressed in the previous paragraph, we admit that the contact network is not a static structure, but evolves in response to the epidemiological state of the population.

Agent-based models whose interaction patterns are represented by networks have received increasing attention during the last years, in the analysis of emergent collective behaviour in complex systems

D. H. Zanette and S. Risau Gusmán at
Consejo Nacional de Investigaciones Científicas y Técnicas, Centro Atómico Bariloche and Instituto Balseiro,
8400 San Carlos de Bariloche, Río Negro, Argentina
Tel.: +54-2944-445173
Fax: +54-2944-445299
E-mail: zanette@cab.cnea.gov.ar, srisau@cab.cnea.gov.ar

[4]. Frequently, the evolution of the interaction network and the dynamics of individual agents occur over different time scales. In learning processes, for instance, connections change adaptively over scales that are large as compared with the internal dynamics of agents [5]. At the opposite limit, in models of network growth, the pattern evolves in the absence of any dynamics related to the agents [4]. When, on the other hand, the dynamical time scales of a population of agents and its interaction network are comparable, we can speak about their *coevolution* [6, 7, 8, 9, 10]. In this context, the model considered in the present study can be regarded as an illustration of the coevolution of agents and networks, inspired in the dynamics of infection spreading.

Our model is based on an SIS epidemiological process where, at a given time, each agent can be susceptible (S) or infected (I). In the standard SIS process, each I-agent spontaneously recovers and becomes susceptible at a fixed rate, say, with probability γ per unit time. An S-agent, in turn, becomes infected by contagion from his infected neighbours. If the contagion probability per unit time and per infected neighbour is ρ , an S-agent with k_I infected neighbours becomes itself infected with probability

$$p_I dt = 1 - (1 - \rho dt)^{k_I} \rightarrow k_I \rho dt \quad (1)$$

during the interval dt . Within a mean-field description, if the average number of (both S and I) neighbours per agent is k and the fraction of I-agents is n_I , we have $k_I = kn_I$. The mean-field evolution equation for n_I thus reads

$$\dot{n}_I = -\gamma n_I + \lambda n_I n_S, \quad (2)$$

where $n_S = 1 - n_I$ is the fraction of S-agents, and $\lambda = k\rho$. In this description, for asymptotically long times, n_I vanishes if $\lambda \leq \gamma$. Therefore, the infection is suppressed as time elapses. If, on the other hand, $\lambda > \gamma$, the fraction of infected agents approaches a finite value $n_I^* = 1 - \gamma/\lambda > 0$, and the infection is endemic. The transition between these two regimes occurs through a transcritical bifurcation at $\lambda = \gamma$.

In the following, we complement the standard SIS model with the possibility that the network of contacts changes in response to the infection spreading. Specifically, links between susceptible and infected agents can be broken, and either removed or reconnected to other agents. As expected, we find that this mechanism decreases the infection level, and can eventually suppress the endemic state. With respect to the standard model, however, infection suppression for high rates of contact change occurs through a tangent bifurcation, which in turn gives rise to a bistability regime. In this regime, the infection persists or dies out depending on the initial fraction of infected agents. More unexpectedly, infection suppression does not require a drastic overall change in the network structure, but is reached with a moderate unbalance between the mean number of neighbours of susceptible and infected agents. As we discuss in the final section, these features are robust under several variations of the dynamical rules.

2 Evolution of the network of contacts: Link removal

We address first the case where before the interaction between an S-agent and an I-agent joined by a network link effectively takes place, so that contagion becomes possible, they may decide to definitively delete that link, thus avoiding any further contact. In this situation, as far as the number of I-agents does not vanish, the network of contacts keeps losing its links. According to our discussion of the standard SIS model (2), however, we expect that when the number of neighbours per agent has decreased sufficiently, the infection dies out. Once no I-agent remains in the population, removal of links stops and the system reaches a static, fully healthy state. To quantify the mechanism of link removal, we assume that each link between an S-agent and an I-agent is deleted with probability q per time unit.

Our formulation of the dynamics of the present model is analogous to the mean-field approach used to derive Eq. (2). We assume that the population consists of N agents, and call N_I and N_S the number of I and S-agents, respectively, so that $N = N_I + N_S$. Additionally, we must introduce new variables to describe the structural state of the network and its relation with the epidemiological state of the population. Therefore, we consider the quantities M_{II} , M_{IS} , and M_{SS} , respectively, the number of network links joining two infected agents (II), an infected agent and a susceptible agent (IS), and two susceptible agents (SS). The total number of links is $M = M_{II} + M_{IS} + M_{SS}$. Due to removal of IS-links, the average change in M_{IS} per time unit is

$$\dot{M}_{IS} = -qM_{IS}. \quad (\text{link removal}) \quad (3)$$

The processes of recovery and infection are the same as discussed for the standard SIS model (2) in the Introduction. Recovery of an I-agent occurs with probability γ per unit time and, for each S-agent, the infection probability per unit time and per infected neighbour is ρ . In a recovery event, when an I-agent becomes susceptible, there is not only a decay in the number of I-agents, but also a change in M_{II} , M_{IS} , and M_{SS} . In fact, the links joining the recovered agent with I and S-agents pass, respectively, from the II-type to the IS-type, and from the IS-type to the SS-type. The number of links of each type associated to a given agent is calculated using mean-field-like averages. For instance, the number of II-links associated to an I-agent is estimated as $2M_{II}/N_I$. Similarly, the number of IS-links associated to an I-agent is M_{IS}/N_I . Using this kind of arguments, we obtain, for each variable, the average change per time unit due to recovery:

$$\begin{aligned}\dot{N}_I &= -\dot{N}_S = -\gamma N_I, \\ \dot{M}_{II} &= -2\gamma M_{II}, \\ \dot{M}_{IS} &= 2\gamma M_{II} - \gamma M_{IS}, \\ \dot{M}_{SS} &= \gamma M_{IS}.\end{aligned}\quad (\text{recovery}) \quad (4)$$

Note that $\dot{M}_{II} + \dot{M}_{IS} + \dot{M}_{SS} = 0$, because recovery events do not change the number of network links.

To calculate the contribution of infection events in the mean-field approximation, we must evaluate the average number of infected neighbours of a susceptible agent. For a randomly chosen S-agent, this number is given by the ratio M_{IS}/N_S . However, it should be taken into account that, to become infected by contagion, a susceptible agent must have at least one infected neighbour. This would restrict the calculation of the number of infected neighbours to those S-agents with at least one IS-link. For the sake of simplicity, we shall still estimate the average number of infected neighbours per S-agent as the above ratio, with the proviso that the approximation is valid when the overall number of I-agents is not too small, so that contagion is in principle possible for all S-agents. The change per time unit due to infection for each variable turns out to be

$$\begin{aligned}\dot{N}_I &= -\dot{N}_S = \rho M_{IS}, \\ \dot{M}_{II} &= \rho M_{IS}^2/N_S, \\ \dot{M}_{IS} &= \rho(2M_{SS} - M_{IS})M_{IS}/N_S, \\ \dot{M}_{SS} &= -2\rho M_{SS}M_{IS}/N_S.\end{aligned}\quad (\text{infection}) \quad (5)$$

Again, $\dot{M}_{II} + \dot{M}_{IS} + \dot{M}_{SS} = 0$.

To obtain differential equations of the type of Eq. (2), it is convenient to define the fractions $n_i = N_i/N$ and $m_{ij} = M_{ij}/M$, with $\{i, j\} \equiv \{I, S\}$. In calculating the variation of m_{ij} per time unit, we must take into account that also the total number of links M varies with time:

$$\dot{m}_{ij} = \frac{\dot{M}_{ij}}{M} - \frac{M_{ij}}{M^2} \dot{M}. \quad (6)$$

Since the total number of links changes by the removal of IS-links only, we have $\dot{M} = -qM_{IS}$. On the other hand, the total number of agents N remains constant. Also, by definition, we have $n_I + n_S = 1$ and $m_{II} + m_{IS} + m_{SS} = 1$, so that we can limit ourselves to study the evolution of n_I , m_{II} , and m_{IS} .

The evolution equations resulting from the above considerations are

$$\begin{aligned}n_I' &= -n_I + \tilde{\lambda}m_{IS}, \\ m_{II}' &= -2m_{II} + \tilde{\lambda}n_S^{-1}m_{IS}^2 + \tilde{q}m_{II}m_{IS}, \\ m_{IS}' &= 2m_{II} - (1 + \tilde{q})m_{IS} + \tilde{\lambda}n_S^{-1}m_{IS}(2m_{SS} - m_{IS}) + \tilde{q}m_{IS}^2,\end{aligned}\quad (7)$$

where primes indicate differentiation with respect to the rescaled time $t' = \gamma t$. We have also defined

$$\tilde{q} = q/\gamma, \quad \tilde{\lambda} = k\rho/2\gamma, \quad (8)$$

where $k = 2M/N$ is the overall mean number of neighbours per agent. Note that, since the number of links M varies with time, the coefficient $\tilde{\lambda}$ is itself time-dependent. Its evolution is determined by the variation of M , and obeys

$$\tilde{\lambda}' = -\tilde{q}m_{IS}\tilde{\lambda}. \quad (9)$$

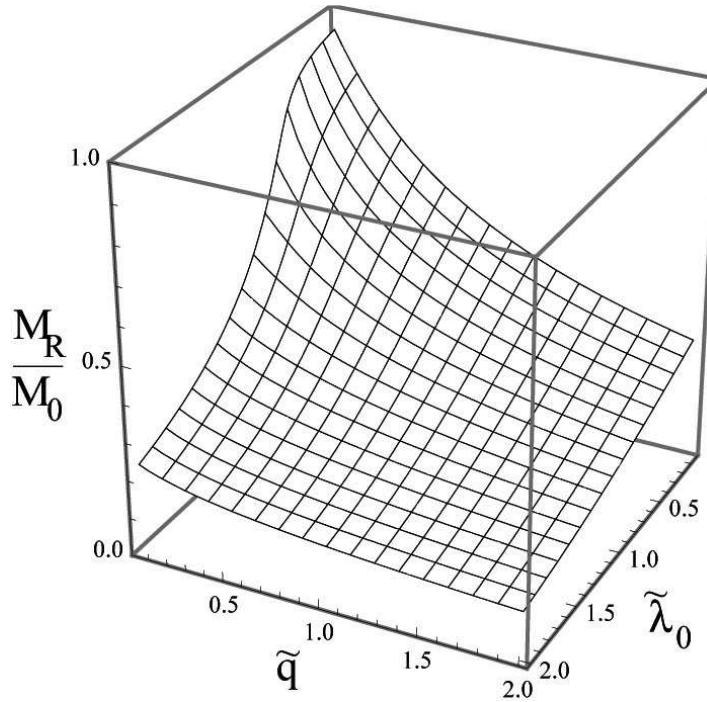


Fig. 1 Number of remaining links, M_R , relative to the initial number of links M_0 , as a function of the normalized removal probability \tilde{q} and initial infectivity $\tilde{\lambda}_0$, for an initial condition where all agents are infected and the population is fully connected.

The numerical solution of Eqs. (7) and (9) confirms the expectation that the infection dies out as a consequence of the sustained removal of links. The fraction of infected agents asymptotically vanishes with time and, accordingly, m_{II} and m_{IS} also tend to zero. Meanwhile, the total number of links approaches a constant M_R . The number of remaining links M_R depends both on the initial number of links, M_0 , and on the initial fraction of infected agents. In fact, for a given rate of link removal, the suppression of a higher initial infection level is expected to take longer times and require more removed links.

Figure 1 illustrates the dependence of the remaining fraction of links, M_R/M_0 , on the normalized rate of link removal \tilde{q} and on the infectivity. The infectivity is here characterized by the initial value of $\tilde{\lambda}$, $\tilde{\lambda}_0 = k_0\rho/2\gamma$, with $k_0 = 2M_0/N$. The results correspond to an initial condition with a fully infected population, $n_I(0) = 1$, and a fully connected network, $M_0 = N(N-1)/2$, so that $m_{II} = 1$ and $m_{IS} = m_{SS} = 0$. As expected, the fraction of remaining links decreases both with $\tilde{\lambda}_0$ and \tilde{q} . Higher infectivities require that a larger fraction of contacts is deleted before the infection dies out, and a larger removal probability contributes in the same direction.

From the viewpoint of the dynamics, the case considered so far –where links keep being removed as long as a fraction of the population remains infected– is not especially interesting. In particular, the transition between infection suppression and persistence observed for $q = 0$ when the infectivity grows, disappears as soon as the removal probability becomes positive. In a real population, moreover, it is expected that discontinued contacts are replaced, at least to some extent, by new social links, in such a way that the structure of society is not too much deteriorated. In the next section, we study a model where links between susceptible and infected agents are not permanently removed, but rather reconnected to other members of the population. Under these conditions, both infection suppression and the endemic state are possible, and can even coexist for a given set of parameters. The dynamics is accordingly richer, and new critical phenomena separating both regimes appear.

3 Reconnection of links

We consider now that, before each susceptible-infected interaction –possibly leading to contagion– takes place, the susceptible agent is given the opportunity of breaking the contact with his infected neighbour and to reconnect the corresponding link to another agent, randomly chosen from the rest of the population. Reconnection of each IS-link occurs with probability r per time unit. If the susceptible agent is reconnected to another susceptible agent, the link changes from the IS-type to the SS-type. Otherwise, no change occurs.

A similar model was considered recently [12] where, however, reconnection of S-agents always occurs towards other S-agents. In this model, upon reconnection, IS-links always change to SS-links. This variant is implicitly admitting that agents have information on the (S or I) state of their equals before making contact, which seems to be a rather artificial assumption. On the other hand, in our model reconnection is done at random, which overcomes such assumption but, at the same time, limits the efficiency of I-agent isolation.

Only the variables M_{IS} and M_{SS} change due to reconnection events. Since the probability of choosing an S-agent at random is n_S we have, per unit time,

$$\dot{M}_{IS} = -\dot{M}_{SS} = -rn_S M_{IS}. \quad (\text{link reconnection}) \quad (10)$$

Changes due to recovery and infection are the same as in Eqs. (4) and (5), respectively.

Obtaining the evolution equations for the fractions n_I , m_{II} , and m_{IS} , is now simpler than in the case of link deletion, because the total number of links M remains constant. We find

$$\begin{aligned} n_I' &= -n_I + \tilde{\lambda} m_{IS}, \\ m_{II}' &= -2m_{II} + \tilde{\lambda} n_S^{-1} m_{IS}^2, \\ m_{IS}' &= 2m_{II} - (1 + \tilde{r} n_S) m_{IS} + \tilde{\lambda} n_S^{-1} m_{IS} (2m_{SS} - m_{IS}). \end{aligned} \quad (11)$$

Here, again, primes indicate differentiation with respect to the rescaled time $t' = \gamma t$. Moreover,

$$\tilde{r} = r/\gamma, \quad \tilde{\lambda} = k\rho/2\gamma, \quad (12)$$

with $k = 2M/N$ the average number of neighbours per agent. Since, now, M does not vary with time, both k and $\tilde{\lambda}$ are constants. Note that the normalized reconnection probability \tilde{r} and infectivity $\tilde{\lambda}$ are the only parameters of Eqs. (11). The normalized infectivity incorporates the only network-specific feature, namely, the mean connectivity k .

3.1 Infection level at equilibrium

We focus the attention on the equilibrium solutions of Eqs. (11), which are the candidates to represent the infection level and network structure at asymptotically long times. First, we consider the stationary values of the fraction of infected agents. The analysis is restricted to the case of $\tilde{\lambda} > 1/2$ which, in the absence of reconnection events ($r = 0$), corresponds to an endemic infection, $n_I > 0$ for $t \rightarrow \infty$ (cf. the discussion of the standard SIS model in the Introduction).

At the fixed points of Eqs. (11), the equilibrium fractions of links m_{II}^* and m_{IS}^* are related to the equilibrium fraction of infected agents n_I^* as

$$m_{II}^* = \frac{n_I^{*2}}{2\tilde{\lambda}(1 - n_I^*)}, \quad m_{IS}^* = \frac{n_I^*}{\tilde{\lambda}}. \quad (13)$$

In turn, n_I^* satisfies

$$0 = n_I^* \left[2\tilde{\lambda} - 1 - \tilde{r} + (3\tilde{r} - 2\tilde{\lambda})n_I^* - 3\tilde{r}n_I^{*2} + \tilde{r}n_I^{*3} \right]. \quad (14)$$

This polynomial equation has four solutions. One of them tends to infinity for $\tilde{r} \rightarrow 0$, and remains real and larger than one for any positive \tilde{r} . Since meaningful solutions to our problem must verify $n_I^* \leq 1$, we disregard this solution from now on.

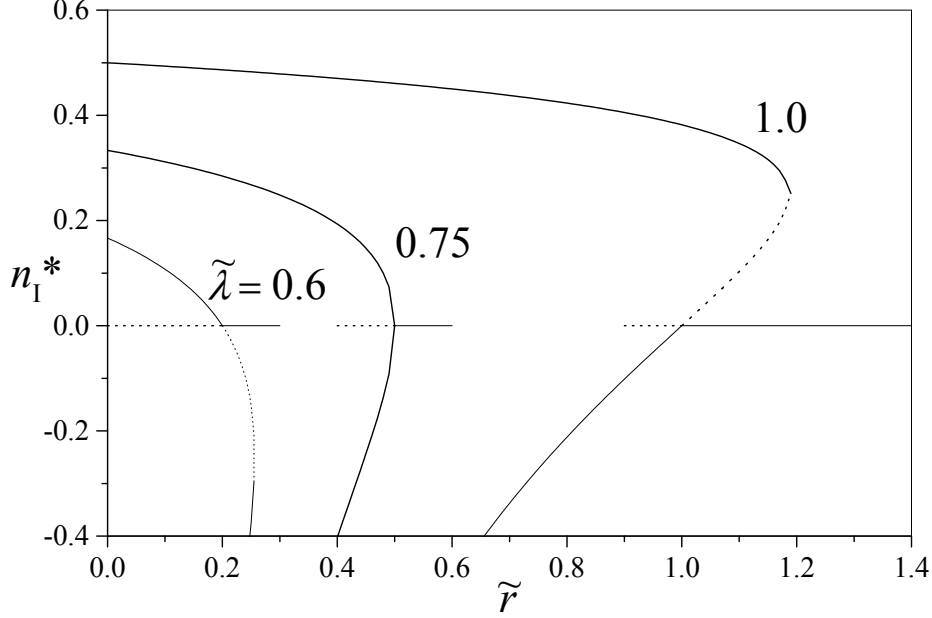


Fig. 2 Bifurcation diagram for the equilibrium fraction of infected agents n_I^* as a function of the normalized reconnection probability \tilde{r} , for three normalized infectivities $\tilde{\lambda}$. Although only positive values of n_I^* are meaningful, an interval in the negative domain is also shown for completeness. Full and dotted lines represent, respectively, stable and unstable branches. For clarity, the solution $n_I^{(0)} = 0$ is plotted in the vicinity of the transcritical bifurcation only.

The trivial solution $n_I^{(0)} = 0$ exists for any value of the normalized infectivity $\tilde{\lambda}$ and of the normalized reconnection probability \tilde{r} . For a given $\tilde{\lambda}$, its stability depends on \tilde{r} . As discussed in more detail below, $n_I^{(0)} = 0$ is unstable for small \tilde{r} and becomes stable as \tilde{r} grows. The other two solutions read

$$n_I^{(1,2)} = 1 - \sqrt{\frac{2\tilde{\lambda}}{3\tilde{r}}} \left[\cos \frac{\alpha}{3} \mp \sqrt{3} \sin \frac{\alpha}{3} \right], \quad (15)$$

with

$$\alpha = \arctan \sqrt{\frac{32\tilde{\lambda}^3}{27\tilde{r}} - 1} \quad (16)$$

($0 \leq \alpha \leq \pi/2$). These two solutions are real for $32\tilde{\lambda}^3 \geq 27\tilde{r}$. Otherwise, they are complex conjugate numbers. The solution $n_I^{(1)}$, with the minus sign in the right-hand side of Eq. (15), approaches $1 - (2\tilde{\lambda})^{-1}$ for $\tilde{r} \rightarrow 0$. Thus, it represents the expected fraction of infected agents in the absence of reconnection. When it is real, it satisfies $n_I^{(1)} < 1$, and it is stable as long as it remains positive. Consequently, along with the trivial solution, $n_I^{(1)}$ is another meaningful equilibrium solution to our problem. Finally, $n_I^{(2)}$ is negative and stable for small \tilde{r} . Depending on $\tilde{\lambda}$, it can become positive as \tilde{r} grows but, at the same time, it becomes unstable. Therefore, it does not represent a meaningful solution.

Figure 2 summarizes, in a bifurcation diagram, the behaviour of $n_I^{(0)}$, $n_I^{(1)}$, and $n_I^{(2)}$ as functions of the normalized reconnection probability \tilde{r} , for three representative values of the normalized infectivity $\tilde{\lambda}$. In the three cases, we have $\tilde{\lambda} > 1/2$, so that –as discussed above– a non-trivial meaningful solution does exist. Full and dotted lines represent, respectively, stable and unstable branches. For small infectivity ($\tilde{\lambda} = 0.6$), the stable solution $n_I^{(1)}$ crosses $n_I^{(0)}$ and becomes negative and unstable, while $n_I^{(0)}$ becomes stable. This transcritical bifurcation takes place at $\tilde{r} = 2\tilde{\lambda} - 1$. As \tilde{r} grows further, $n_I^{(1)}$ and the negative stable solution $n_I^{(2)}$ approach each other, and collide when $n_I^{(1)} = n_I^{(2)} = 1 - 3/4\tilde{\lambda}$. Beyond this tangent bifurcation, which takes place at $\tilde{r} = 32\tilde{\lambda}^3/27$, the two solutions are complex numbers.

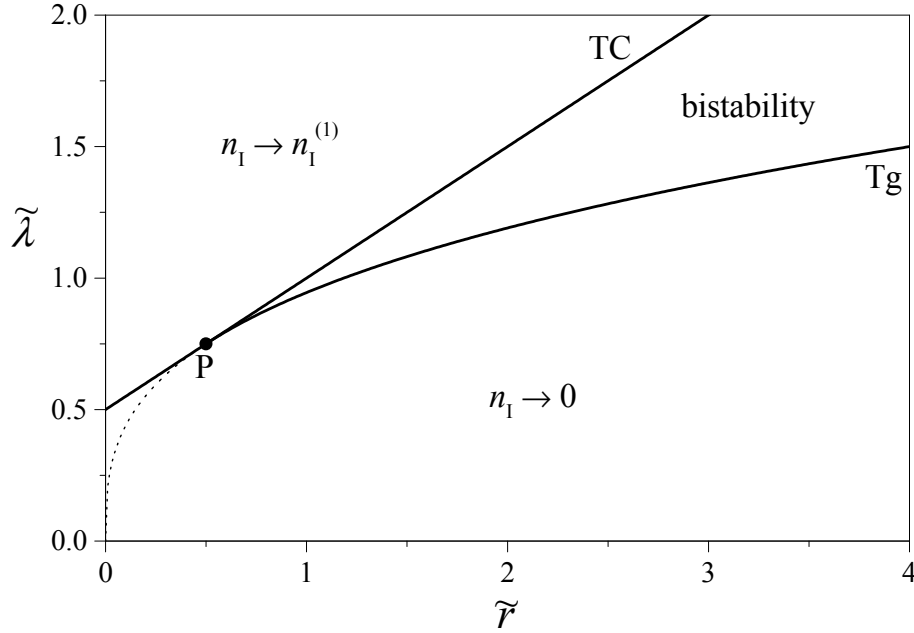


Fig. 3 Phase diagram in the $(\tilde{r}, \tilde{\lambda})$ -plane, showing the regions of infection suppression ($n_I \rightarrow 0$) and persistence ($n_I \rightarrow n_I^{(1)}$), and the intermediate bistability zone. Their boundaries are given by the transcritical (TC) and the tangent (Tg) bifurcation lines, which collapse into a pitchfork bifurcation (P) at $(1/2, 3/4)$. The dotted line is the continuation of the tangent bifurcation line in the zone where $n_I^{(1)}$ is negative.

The situation is different for larger infection probabilities, as illustrated by Fig. 2 for $\tilde{\lambda} = 1$. Now, for $\tilde{r} = 0$, $n_I^{(1)}$ is large and, as \tilde{r} grows, it is the stable negative solution $n_I^{(2)}$ which first reaches $n_I^{(0)}$. At the transcritical bifurcation at $\tilde{r} = 2\tilde{\lambda} - 1$, $n_I^{(2)}$ becomes positive and unstable, and $n_I^{(0)}$ becomes stable. The tangent bifurcation where $n_I^{(1)}$ and $n_I^{(2)}$ collide and become complex, at $\tilde{r} = 32\tilde{\lambda}^3/27$, takes now place when these two solutions are positive. As a consequence, there is an interval of normalized reconnection probabilities, between the two bifurcations, where the system is bistable: both $n_I^{(0)}$ and $n_I^{(1)}$ are stable meaningful solutions to the problem. The asymptotic state is selected by the initial condition for n_I .

The regimes of small and large infectivity are separated by the critical value $\tilde{\lambda} = 3/4 = 0.75$, also shown in Fig. 2. At this critical point, the transcritical bifurcation and the tangent bifurcation collapse into a pitchfork bifurcation at $\tilde{r} = 1/2$. Here, the three equilibria collide simultaneously, and $n_I^{(0)}$ becomes stable, while the other two solutions become complex.

A phase diagram of our system over the parameter plane $(\tilde{r}, \tilde{\lambda})$ is shown in Fig. 3. The zones of endemic infection, where the fraction of infected agents at asymptotically long times is positive ($n_I \rightarrow n_I^{(1)}$), and of infection suppression ($n_I \rightarrow 0$) are separated, for large $\tilde{\lambda}$ and \tilde{r} , by the bistability region, where the two asymptotic behaviours can be obtained, depending on the initial condition. The three zones are limited by the lines of the transcritical bifurcation [$\tilde{\lambda} = (1 + \tilde{r})/2$, TC], where $n_I^{(0)} = 0$ changes its stability, and of the tangent bifurcation [$\tilde{\lambda} = (27\tilde{r}/32)^{1/3}$, Tg] where $n_I^{(1)}$ and $n_I^{(2)}$ collide and become complex. These two lines are tangent to each other at the “triple point” $(1/2, 3/4)$, where the bistability region disappears, and the system undergoes a pitchfork bifurcation [P]. For smaller $\tilde{\lambda}$ and \tilde{r} bistability is no more possible, and the zones of infection persistence and suppression are separated by the transcritical line. The tangent bifurcation takes now place at negative values of $n_I^{(1)}$ and $n_I^{(2)}$ (dotted line).

Let us summarize our results on the persistence or suppression of the infection in terms of the non-normalized parameters. First, for small infectivity, $\rho \leq \gamma/k$, the infection is always suppressed. In this situation, the infectivity is just too small to sustain a finite infected population. For larger infectivities,

on the other hand, the infection can become established, depending on the reconnection probability r . In the range $\gamma/k < \rho < 3\gamma/2k$, the infection is endemic if reconnections are infrequent, $r < k\rho - \gamma$. Otherwise, for sufficiently frequent reconnections, the infection dies out. The transition between the two situations is continuous in the fraction of infected agents, and occurs through a transcritical bifurcation. For even larger infection probabilities, $\rho > 3\gamma/2k$, the regimes of persistence (low r) and suppression (large r) are separated by a bistability zone, where the infection persists or dies out depending on the initial fraction of infected agents. The bistability zone is limited by the transcritical bifurcation quoted above and a tangent bifurcation at a reconnection probability $r = 4k^3\rho^3/27\gamma^2$. The discontinuous nature of the tangent bifurcation implies that the endemic state present in the bistability zone disappears abruptly at the boundary, with a finite jump in the asymptotic fraction of infected agents, from $n_I = 1 - \sqrt{k\rho/3r} > 0$ to zero.

3.2 Number of neighbours of infected and susceptible agents

The variables m_{II} and m_{IS} characterize how the structure of the network is related to the state of the agents. Reconnection events favor the growth of the number of SS-links at the expense of IS-links. Thus, for $r > 0$, S-agents should asymptotically possess relatively large numbers of neighbours. The equilibrium values m_{II}^* and m_{IS}^* as functions of the equilibrium fraction n_I^* of I-agents are given by Eqs. (13). These equations show, as expected, that the fraction of links connecting I-agents with any other agent is proportional to the fraction of I-agents itself.

In order to introduce quantities that define the connectivity of I-agents and S-agents independently of their respective fractions, we consider the average number of neighbours per agent of each type. For I-agents, for instance, the average numbers of infected and susceptible neighbours are $2M_{II}/N_I$ and M_{IS}/N_I , respectively. The average connectivity of I-agents, k_I , is the sum of these two quantities or, equivalently,

$$\frac{k_I}{k} = \frac{1}{2\tilde{\lambda}(1 - n_I^*)}, \quad (17)$$

which gives the ratio between k_I and the overall average connectivity per agent, $k = 2M/N$. With analogous arguments for S-agents, their average connectivity reads

$$\frac{k_S}{k} = \frac{1}{1 - n_I^*} - \frac{n_I^*}{2\tilde{\lambda}(1 - n_I^*)^2}. \quad (18)$$

Due to the conservation of the total number of links, k_I and k_S are univocally related. This relation can be obtained from Eqs. (17) and (18) by eliminating n_I^* , which yields

$$k_S = k_I[1 + 2\tilde{\lambda}(1 - k_I/k)]. \quad (19)$$

In order to describe the correlation between the structure and the state of the population it is however useful to analyze both k_I and k_S as functions of the relevant parameters. Figure 4 illustrates the behaviour of k_I and k_S , as described in the following, for the infection probabilities $\tilde{\lambda}$ already considered in Fig. 2.

For $n_I^* = n_I^{(1)}$, which stands for the stable equilibrium solution for low reconnection probabilities, both k_I and k_S approach k as $\tilde{r} \rightarrow 0$. As expected, in the absence of reconnection events, there is no difference in the number of neighbours of infected and susceptible agents. As \tilde{r} grows from zero, we have $k_I < k < k_S$. We thus verify that reconnection tends to increase the connectivity of S-agents at the expense of I-agents.

The other solution relevant to the process, $n_I^* = n_I^{(0)} = 0$, corresponds to a purely susceptible population. Accordingly, we find $k_S = k$. Note also that Eq. (17) predicts $k_I = k/2\tilde{\lambda}$, but this value is never realized due to the total absence of I-agents in this state.

For $\tilde{\lambda} \leq 3/4$, the fraction of I-agents decreases monotonically with \tilde{r} and vanishes continuously at the transcritical bifurcation –or, for $\tilde{\lambda} = 3/4$, at the pitchfork bifurcation. The connectivity of S-agents is $k_S = k$ both at $\tilde{r} = 0$ and at the bifurcation. For intermediate values of the reconnection probability k_S is larger than k and attains a maximum. This maximum, which at first glance may seem surprising, can be easily explained. In fact, to sustain a value of k_S larger than the overall average k , it is necessary

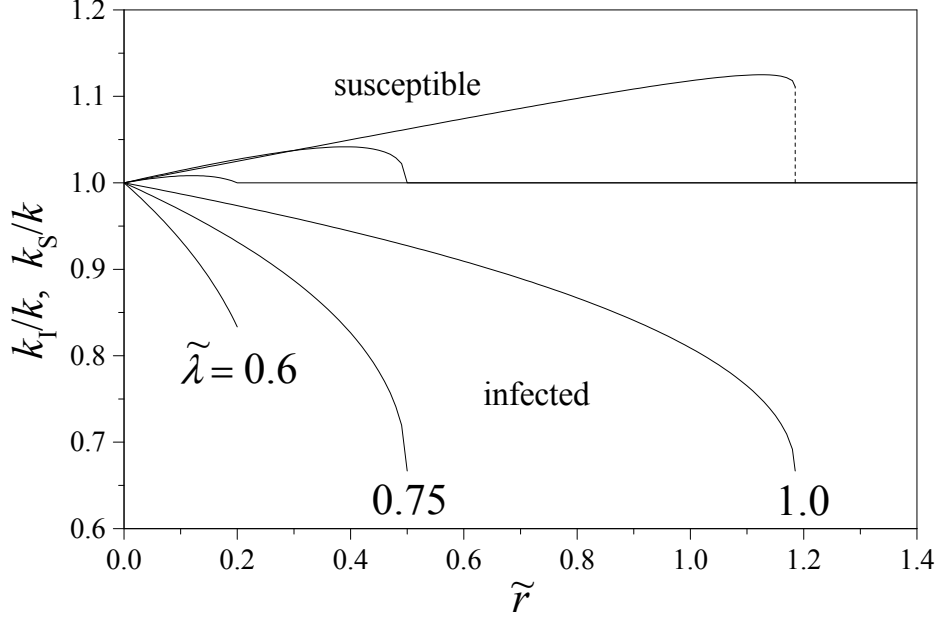


Fig. 4 Connectivity of infected and susceptible agents, k_I and k_S , relative to the overall connectivity $k = 2M/N$, for three values of the normalized infectivity $\tilde{\lambda}$, as functions of the normalized reconnection probability \tilde{r} . Only the values corresponding to meaningful stable solutions for the fraction of infected agents are plotted. The connectivity of infected agents is not plotted beyond the threshold of infection suppression. The vertical dashed line represents the finite jump in k_S at the tangent bifurcation where the solution $n_I^{(1)}$ disappears.

to have I-agents with a relatively low number of neighbours. As the infection is progressively suppressed by reconnection, the number of I-agents decreases and, accordingly, their contribution to the average number of neighbours per agent becomes less significant. At the bifurcation and beyond, S-agents must account for the whole average, so that k_S returns to its value for $\tilde{r} = 0$, i.e. $k_S = k$.

The connectivity of I-agents, in turn, is a monotonically decreasing function of \tilde{r} , and reaches $k_I = k/2\tilde{\lambda} < k$ at the bifurcation. This implies that, even at the threshold of infection suppression, I-agents maintain a finite number of neighbours within the population.

For $\tilde{\lambda} > 3/4$, again, the connectivity k_S associated with the solution $n_I^{(1)}$ initially increases with \tilde{r} , and attains a maximum. In the subsequent decay, however, it does not reach $k_S = k$. In fact, $n_I^{(1)}$ disappears through a tangent bifurcation when it is still positive, so that the jump in the infection level is discontinuous. At the bifurcation, we find $k_S = 2k(2\tilde{\lambda} + 3)/9 > k$. The connectivity of I-agents decreases with \tilde{r} and, at the bifurcation, its value is independent of $\tilde{\lambda}$: $k_I = 2/3$.

From the viewpoint of the interplay of the epidemiological dynamics and the structure of the underlying network, the most interesting result of this analysis is the fact that the infection dies out even when infected agents keep a substantial connectivity with the rest of the population. In the cases illustrated in Fig. 4, for instance, infected agents preserve more than 60 % of their connections at the threshold where the infection level vanishes. In other words, as we had already verified for link deletion, reconnection needs not to completely isolate infected agents to suppress the infection. A moderate, partial isolation of the infected population is enough to asymptotically inhibit the endemic state.

4 Heuristic description of infection suppression by link reconnection

What mechanisms are at work when the infection is suppressed by reconnection, even when the connectivity of infected agents remains fairly high? To advance an answer to this question, it helps to consider a simpler dynamical system for the fraction of I-agents:

$$n_I' = -n_I + [2\tilde{\lambda} - \tilde{r}(1 - n_I)^2]n_I(1 - n_I). \quad (20)$$

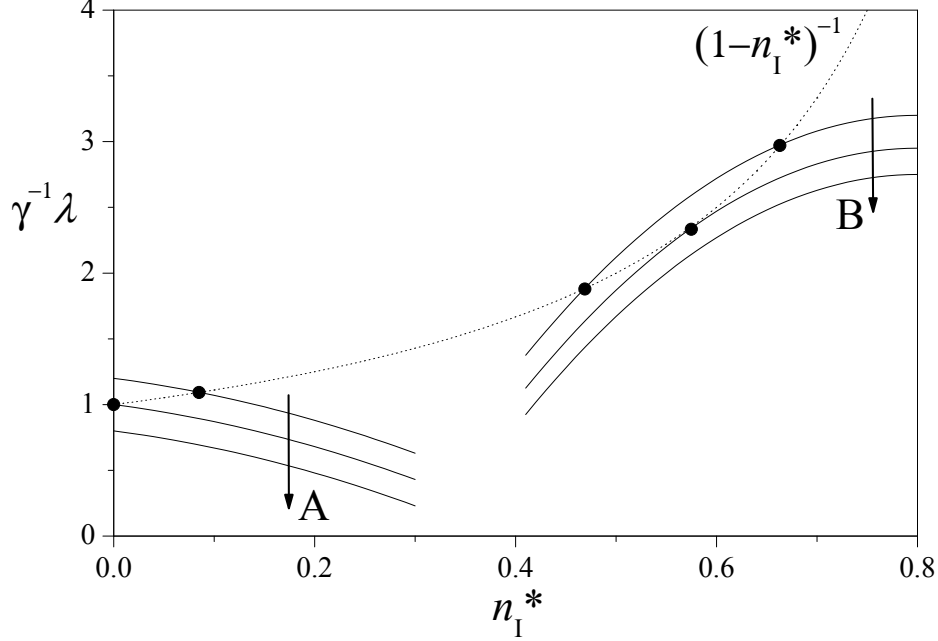


Fig. 5 Graphical solution of Eq. (23). The dotted curve represents the right-hand side of the equation, and full curves are possible graphs of the left-hand side. Dots stand at their intersections. The arrows illustrate how the graphs may change upon the variation of parameters, in the cases of a transcritical bifurcation (A) and of a tangent bifurcation (B).

The right-hand side of this equation is just a rearrangement of that of Eq. (14). The equilibria of Eq. (20) are thus identical to the equilibria for n_I in Eqs. (11). Moreover, their stability properties are also the same as in our original system. It is important to understand, however, that (20) and (11) are not equivalent: they merely share the same equilibrium behaviour in what regards the fraction of I-agents.

We immediately see that Eq. (20) can be put in the form of the standard mean-field equation (2) for a SIS process if we introduce the effective infection probability

$$\lambda_{\text{eff}} = \gamma[2\tilde{\lambda} - \tilde{r}(1 - n_I)^2] = (1 - r)k\rho - r(1 - n_I)^2. \quad (21)$$

In Eq. (2) the threshold of infection suppression, where the trivial equilibrium changes its stability, is given by $\lambda = \gamma$. Imposing this same condition to λ_{eff} , we find $\tilde{r} = 2\tilde{\lambda} - 1$. But this is precisely the suppression threshold in the system with reconnections. Therefore, with respect to the stabilization of the trivial equilibrium, the system (11) is effectively equivalent to the standard SIS model with infectivity λ_{eff} . The transcritical bifurcation of Eqs. (11), where $n_I^{(0)} = 0$ becomes stable, can be interpreted as a kind of continuation for $r \neq 0$ of the transcritical bifurcation of the SIS model without reconnection events.

The interpretation of the tangent bifurcation where the endemic state disappears at a positive value of $n_I^{(1)}$, for $\tilde{\lambda} > 3/4$, is less direct. It can however be argued that the presence of such a bifurcation, together with the transcritical bifurcation which stabilizes the trivial equilibrium, constitutes the most generic critical behaviour expected for an epidemiological model like Eq. (2) when the infection probability depends on the density of I-agents:

$$n_I' = -\gamma n_I + \lambda(n_I)n_I(1 - n_I). \quad (22)$$

Besides the trivial equilibrium, this equation has fixed points at the solutions of

$$\gamma^{-1}\lambda(n_I^*) = (1 - n_I^*)^{-1}. \quad (23)$$

Figure 5 illustrates graphically two representative situations. The dotted curve is the graph of the right-hand side of Eq. (23) as a function of n_I^* . If the graph of $\gamma^{-1}\lambda(n_I^*)$ has a single intersection with

the dotted curve (A) and if, upon variation of parameters in the infection probability, the graph varies as indicated by the arrow, the intersection crosses $n_I^* = 0$ and a transcritical bifurcation takes place. The standard SIS model, in which λ is constant, is an example of this situation. More generally, the graph of $\gamma^{-1}\lambda(n_I^*)$ may have two (B) or more intersections with the dotted curve. When the parameters change, it is still possible that one of the intersections becomes involved in a transcritical bifurcation crossing $n_I^* = 0$, as in situation A. Now, however, it may well be the case that two intersections approach each other, and eventually collapse and disappear, as in B. In this case, Eq. (22) undergoes a tangent bifurcation, as found to happen in our system (11).

In summary, the above discussion shows that the suppression of the endemic state as a result of reconnection events can be heuristically understood in terms of the critical behaviour of a standard SIS model with an effective infectivity, which depends on both the reconnection probability and on the fraction of infected agents. The transcritical bifurcation which stabilizes the state where the infection is completely inhibited is interpreted as a continuation of a similar transition in the absence of reconnection. In turn, the tangent bifurcation –which, for large infectivities, suppresses the infection as the reconnection probability grows– is a generic phenomenon in SIS models with density-dependent infectivity [13].

5 Conclusion

In this paper, we have studied a model for an SIS epidemiological process in a population of agents on a network, where contagion can occur along the network links. The network coevolves with the population as the infection progresses: as a response to risk perception, susceptible agents can decide to break links with their infected peers. In the first version of the model, broken links are permanently removed from the network. For any positive probability of link removal, the infection is found to asymptotically die out. During the process, a fraction of network links is deleted, so that the social structure is degraded in the long-time limit. As expected, the fraction of remaining links decreases as the removal probability and the infectivity grow.

In the second version, a susceptible agent who has broken a link with an infected agent reconnects it to a randomly chosen member of the remaining population. In this case, whether the infection persists or is asymptotically suppressed depends on the reconnection probability. Suppression of the endemic state does not require full isolation of the infected population. On the contrary, it can be achieved while each infected agent preserves a substantial part of the links with the rest of the population.

Reconnection of network links introduces new dynamical features with respect to the standard SIS process. In particular, for sufficiently high reconnection probabilities, the continuous transition associated with infection suppression is replaced by a discontinuous tangent bifurcation, where the infected fraction of the population drops abruptly as the relevant parameters are changed. The appearance of this new critical phenomenon is accompanied by the creation of a bistability regime, where the infection can either persist or die out depending on the initial fraction of infected agents.

These results are remarkably robust under variations of the dynamical rules of the model. Here, for instance, we have assumed that link reconnection occurs, at each time step, before infection events, so that contagion can only take place from those infected agents who have retained their links. If this ordering is altered, the position of the bifurcation –and, consequently, the threshold of infection suppression– change, but the overall qualitative picture of Fig. 3 is not modified. The same holds if reconnected links are kept, with a certain probability, by infected agents, instead of always being susceptible agents which retain broken contacts.

As shown in Section 3, the SIS model with link reconnections can be analytically solved in equilibrium. To a large extent, the possibility of explicitly writing the stationary solution for the density of infected agents and the expression for critical lines in the parameter space is a direct consequence of the approximation done in Section 2, just before Eqs. (5), on the average number of infected neighbours of susceptible agents. As stated there, the approximation is valid as long as the number of infected agents remains high. On the other hand, we have pushed the solution to describe also the regime where the infection dies out. The question thus arises on whether our analytical solution still gives a reasonable description of the epidemiological dynamics. To advance an answer, we have performed agent-based numerical simulations of the SIS process on the evolving network. Results exhibit quantitative differences with the analytical solution, especially in the prediction of the critical points. Those

are precisely the zones where the analytical description is expected to fail, because at those points the infection is suppressed and the approximation breaks down. Qualitatively, however, the numerical and analytical results for the critical behaviour are the same. Simulations confirm the prolongation of the transcritical bifurcation for non-zero reconnection probabilities, and the appearance of the tangent bifurcation, along with the bistability regime, as reconnections become more frequent.

Numerical simulations automatically incorporate further dynamical elements which are not present in a mean-field analytical description, such as the creation of correlations between the relative positions of susceptible or infected agents and the effects of heterogeneity in the distribution of network links. Extensive numerical results, as well as an improved analytical approach able to take into account correlations induced by the spatial structure of the network [15], will be presented in a forthcoming paper [14].

References

1. Hatchett, R. J., Mecher, C. E., Lipsitch, M.: Public health interventions and epidemic intensity during the 1918 influenza pandemic, *Proc. Natl. Acad. Sci. USA* **104**, 7582-7587 (2007).
2. Bootsma, M. C., Ferguson N. M.: The effect of public health measures on the 1918 influenza pandemic in U.S. cities. *Proc. Natl. Acad. Sci. USA* **104**, 7588-7593 (2007).
3. Hurst, C. J.: *Modeling Disease Transmission and its Prevention by Disinfection*. Cambridge University Press, Cambridge (1996).
4. Pastor Satorras, R., Rubi, M., Díaz Guilerá, A.: *Statistical Mechanics of Complex Networks*. Springer, Berlin (2003).
5. Haykin, S.: *Neural Networks: A Comprehensive Foundation*. Prentice Hall, New York (2007).
6. Zimmermann, M. G., Eguíluz, V. M., San Miguel, M.: Coevolution of dynamical states and interactions in dynamic networks, *Phys. Rev. E* **69**, 065102R (2004).
7. Stauffer, D., Hohnisch, M., Pittnauer, S.: The coevolution of individual economic characteristics and socio-economic networks, *Physica A* **370**, 734-740 (2006).
8. Gil, S., Zanette, D. H.: Coevolution of agents and networks: Opinion spreading and community disconnection, *Phys. Lett. A* **356**, 89-94 (2006).
9. Zanette, D. H., Gil, S.: Opinion spreading and agent segregation on evolving networks, *Physica D* **224**, 156-165 (2006).
10. Holme, P., Newman, M. E. J.: Nonequilibrium phase transition in the coevolution of networks and opinions, *Phys. Rev. E* **74**, 056108 (2006).
11. Bagnoli, F., Lio, P., Sguanci, L., Role of risk perception in epidemiological models, arXiv:0705.1974v2 [q-bio.PE].
12. Gross, T., Dommar D'Lima, C., Blasius, B.: Epidemic dynamics on an adaptive network, *Phys. Rev. Lett.* **96**, 208701 (2006).
13. An example is explicitly analyzed in Anderson, R. M., May, R. M., Anderson, B.: *Infectious Diseases of Humans: Dynamics and Control* Oxford University Press, Cambridge (1992).
14. Risau Gusmán, S., Zanette, D. H.: in preparation.
15. Levin, S. A., Durrett, R.: From individuals to epidemics. *Phil. Trans. R. Soc. Lond. B* **351**, 1615-1621 (1996).